The Astrophysical Journal Letters, 962:L21 (7pp), 2024 February 10 https://doi.org/10.3847/2041-8213/ad2463

Eccentricity Distribution beyond the Snow Line and Implications for Planetary Habitability

Stephen R. Kane[1] and Robert A. Wittenmyer[2]
[1] Department of Earth and Planetary Sciences, University of California, Riverside, CA 92521, USA; skane@ucr.edu
[2] University of Southern Queensland, Centre for Astrophysics, West Street, Toowoomba, QLD 4350, Australia
Received 2023 December 29; revised 2024 January 27; accepted 2024 January 31; published 2024 February 9

Abstract

A fundamental question in the study of planetary system demographics is: how common is the solar system architecture? The primary importance of this question lies in the potential of planetary systems to create habitable environments, and dissecting the various components of solar system evolution that contributed to a sustainable temperate surface for Earth. One important factor in that respect is volatile delivery to the inner system and the dependence on giant planets beyond the snow line as scattering agents, particularly as such cold giant planets are relatively rare. Here, we provide an investigation of the eccentricity distribution for giant planet populations both interior and exterior to their system snow lines. We show that the median eccentricity for cold giants is 0.23, compared with a far more circular orbital regime for inner planets. We further present the results of a dynamical simulation that explores the particle scattering potential for a Jupiter analog in comparison with a Jupiter whose eccentricity matches that of the median cold giant eccentricity. These simulations demonstrate that the capacity for such an eccentric cold giant system to scatter volatiles interior to the snow line is significantly increased compared with the Jupiter analog case, resulting in a far greater volume of Earth-crossing volatiles. Thus, many of the known systems with cold giant planets may harbor water worlds interior to the snow line.

Unified Astronomy Thesaurus concepts: Habitable zone (696); Exoplanets (498); Exoplanet systems (484); Exoplanet dynamics (490); Exoplanet evolution (491); Orbits (1184); Orbital evolution (1178); Solar system (1528); Solar system gas giant planets (1191); Solar system evolution (2293)

1. Introduction

Surveys for exoplanet discovery have now been operating for several decades, and have been increasing the sensitivity of such measurements to a greater diversity of exoplanet masses and semimajor axes. For example, radial velocity (RV) surveys have developed long observational baselines (Fischer et al. 2016) that have probed into the outer regions of planetary systems (Wittenmyer et al. 2013). With thousands of exoplanets now known, the distribution of planetary architectures is gradually becoming apparent (Ford 2014; Winn & Fabrycky 2015; He et al. 2019; Mishra et al. 2023). In particular, exoplanet demographics may be compared to the architecture of the solar system in order to place the masses and orbits of our planets within the broader context of planetary formation and evolution (Martin & Livio 2015; Horner et al. 2020; Raymond et al. 2020; Kane et al. 2021a). Such comparisons have revealed that our system may be relatively unusual in the harboring of several giant planets beyond the snow line, since the prevalence of similar planets in other systems appears to be relatively rare, even for solar-type stars (Wittenmyer et al. 2011, 2016, 2020; Fulton et al. 2021; Rosenthal et al. 2021; Bonomo et al. 2023). Since Jupiter is the overwhelming dominant planetary mass within the solar system, it is critically important that we understand the role of giant planets in the evolution of terrestrial planets, especially those that reside within the habitable zone (HZ) of the system (Kasting et al. 1993; Kane & Gelino 2012; Kopparapu et al. 2013, 2014; Kane et al. 2016; Hill et al. 2018, 2023).

Giant planet formation within a protoplanetary disk can result in numerous important planet–planet interactions that can play a dominant role in the sculpting of the eventual planetary architecture (Morbidelli et al. 2007; Raymond et al. 2008, 2009a; Kane 2023a), and can limit the formation and stability of habitable planets (Raymond 2006; Kopparapu & Barnes 2010; Kane 2015, 2023b; Kane et al. 2020). The precise nature of how the presence of giant planets within a system influences the formation of inner planets, the abundance of volatile delivery, and the potential habitability of HZ planets is an active area of research (Morbidelli et al. 2000; Morbidelli & Raymond 2016; Clement et al. 2022). A key consideration is the location of the "snow line," which is the radial distance from the center of a protostellar disk beyond which volatiles (such as water) can efficiently condense to form ice (Ida & Lin 2005; Kennedy et al. 2006; Kennedy & Kenyon 2008; Kane 2011; Ciesla 2014). As giant planets form beyond the snow line, their accretion and migration can lead to significant scattering of volatiles to the inner part of the disk (Raymond & Bonsor 2014; Raymond & Izidoro 2017; Venturini et al. 2020). This scattering effect is a crucial component for forming the volatile inventory of terrestrial planets, most particularly the water mass that can contribute to a sustained presence of surface liquid water (Raymond et al. 2004; Ciesla et al. 2015; Marov & Ipatov 2018; Ogihara et al. 2023). Moreover, the eccentricity of planets beyond the snow line plays a role in the scattering profile of encountered material, and the subsequent prospects for impact scenarios with the inner planets. The solar system giant planets have likely passed through eccentric phases of their orbital evolution via planet–planet interactions and migration processes, before arriving at their present

near-circular orbits (Clement et al. 2021). Exoplanets provide a statistical basis from which to evaluate the eccentricity distribution (Shen & Turner 2008; Hogg et al. 2010; Kane et al. 2012; Sagear & Ballard 2023) and the implications for planet formation scenarios (Jurić & Tremaine 2008; Ida et al. 2013). Given the relative scarcity of their population, giant planets beyond the snow line enable an exploration of the effect of their eccentricity distribution on the disbursement of icy material throughout the system.

Here, we present the results of a comparative study of the eccentricity distribution of giant planets on either side of the snow line, and the dynamical consequences for volatile delivery to the inner region of planetary systems. Section 2 describes the selection criteria for our giant planet sample, and the eccentricity distribution statistics with respect to the snow line. Section 3 provides the results of a dynamical simulation that calculates the fractional amount of injected particles that are scattered interior to the snow line, comparing a Jupiter analog scenario with that of a Jupiter with considerably higher eccentricity. Section 4 discusses the known occurrence rate of cold Jupiters, and the implication of our dynamical results for volatile delivery, planetary habitability, and the frequency of water worlds. Finally, we provide concluding remarks and suggestions for future work in Section 5.

2. Demographics beyond the Snow Line

Here, we describe our sample selection for exploring the eccentricity distribution both interior and exterior to the snow line.

2.1. Sample Selection and Snow Line

Our sample consists of known giant exoplanets detected beyond the snow line of their host stars. The data for our sample were extracted from the NASA Exoplanet Archive (Akeson et al. 2013) and are current as of 2023 October 20 (NASA Exoplanet Archive 2023). We selected all planets with valid (non-null) values for the semimajor axis (a), planet mass (M_p), orbital eccentricity (e), and the mass of the host star ($M_\star$). This provided an initial sample of 1492 planets. We further constrained the data by retaining only those planets whose mass is equal to or greater than Saturn's mass ($\sim$0.3 M_J), which produced a sample size of 846 planets. Finally, we calculated the snow line for each of the host stars in the sample. The location of the snow line was approximated as a function of stellar mass using the relationship $a_{\rm ice} = 2.7(M_\star/M_\odot)^2$, derived by Ida & Lin (2005), and which provides an estimated snow line location of $\sim$2.7 au for the solar case (see Section 3). The sample of planets was divided into those interior to the system snow line (651 planets) and those exterior (195 planets).

2.2. Eccentricity Distribution

Based on the sample selection described in Section 2.1, we examined the planetary property distributions as a function of semimajor axis. The extracted eccentricity data are represented in Figure 1 as a function of semimajor axis, where the planets' interior to the snow line are shown in the left panels, and those exterior to the snow line are shown in the right panels. For the scatter plots shown in the top two panels, both the shade and size of the data points are logarithmically proportional to the planet mass, where dark green and light green indicate planets at the low and high end of the mass range (see Section 2.1), respectively. Note that, since many of the planets included in our sample are nontransiting, many of the masses are minimum masses depending on their orbital inclination relative to the plane of the sky. The data plotted in the top-left panel show the well-known trend toward circular orbits for small star–planet separations (Jurić & Tremaine 2008; Shen & Turner 2008) that largely results from tidal circularization (Goldreich & Soter 1966; Ivanov & Papaloizou 2007). The top panels of Figure 1 also reveal a larger concentration of low-mass planets that lie interior to the snow line. For the planet population interior to the snow line, the mean and median mass values are 2.74 and 1.28 Jupiter masses, respectively. For the planet population exterior to the snow line, the mean and median mass values are 7.64 and 5.15 Jupiter masses, respectively. This difference in mass distribution is in large part caused by the observational bias, both in terms of the survey precision and duration requirements needed to detect similar planets beyond the snow line (Kane et al. 2007; Ford 2008; Wittenmyer et al. 2013).

Of particular interest to our analysis is the eccentricity distribution for those planets either side of the estimated snow line in each system. It is apparent from Figure 1 that the eccentricities shown in the top-right panel are more evenly distributed than those in the top-left panel. Quantitatively, for those planets in our sample that are interior to the snow line, the mean and median eccentricities are 0.18 and 0.01, respectively, with a 1σ rms scatter of 0.21. For those planets exterior to the snow line, the mean and median eccentricities are 0.29 and 0.23, respectively, with a 1σ rms scatter of 0.23. The large difference between mean and median eccentricities for the planets' interior to the snow line suggests the sample is heavily skewed by outliers, dominated by observational bias toward the detection of inner planets and the tidal circularization that occurs within that regime, and can be clearly seen in the histograms shown in the bottom panels of Figure 1. By contrast, the proximity of the mean and median for the sample beyond the snow line indicates a relatively symmetrical distribution of the eccentricities. To quantify these differences more thoroughly, we conducted a null hypothesis Kolmogorov–Smirnov (K-S) test to assess the statistical significance of the similarities between data sets. The K-S test produced a probability of $\sim$0.0, thus rejecting the hypothesis that the two samples are drawn from the same distribution. However, excluding planets with an orbital period of less than 10 days results in a median eccentricity of 0.24 for planets' interior to the snow line, more closely resembling the eccentricity distribution exterior to the snow line. A K-S test using these new criteria resulted in a probability of $\sim$0.997, such that the hypothesis of the two samples being drawn from the same distribution may be accepted. As a further test, we considered the constraints of excluding planets with an orbital period of less than 10 days and also increasing the lower limit on planet mass from 0.3 M_J. The K-S test using these revised samples produced probabilities of 0.646 and 0.327 for lower mass limits of 1.0 M_J and 2.0 M_J, respectively. These results similarly lead to the acceptance that both samples are drawn from the same distribution, though at a lower significance than the 0.3 M_J lower mass limit. These differences in K-S test outcome due to the choice of the lower mass limit are consistent with previous work that found an eccentricity dependency on planet mass (Jones et al. 2006; Ribas & Miralda-Escudé 2007; Ford & Rasio 2008; Wright et al. 2009), which may be due to an

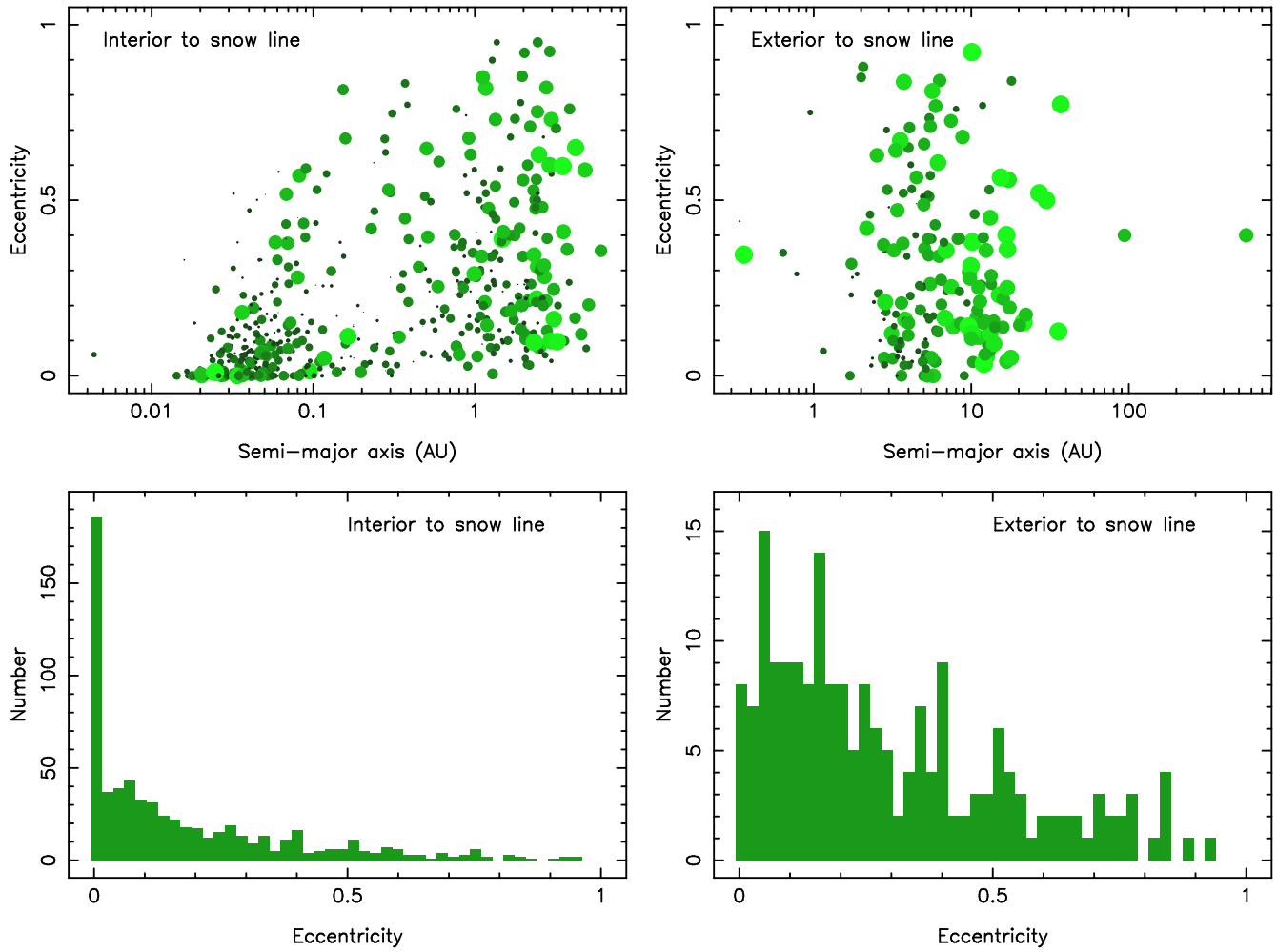

Figure 1. Distribution of eccentricities for all planets more massive than 0.3 M_J interior to the snow line (left panels) and exterior to the snow line (right panels). For the top two panels, both the shade and the size of the plotted data are logarithmically proportional to the planet mass, where dark green indicates a low mass and light green indicates a high mass. The bottom two panels show the histograms of the eccentricity data appearing in the top two panels.

increase in planet–planet scattering events (Raymond et al. 2010; Ida et al. 2013). Thus, our analysis indicates that the differences between the two original samples described in Section 2.1 are largely due to the circularization of short period planets, but also exhibit planet mass dependencies For our subsequent dynamical simulations, we adopt the median eccentricity of the sample beyond the snow line ($e = 0.23$) as a representative example.

3. Dynamical Consequences

An increase in eccentricity for a giant planet beyond the snow line may have a significant effect on the planet's ability to scatter material interior to the snow line. To test the effect of eccentricity on scattering potential, we conducted a series of dynamical simulations that explored the specific case of a Jupiter analog and the equivalent eccentricity case. We used the Mercury Integrator Package (Chambers 1999) with a hybrid symplectic/Bulirsch–Stoer integrator with a Jacobi coordinate system (Wisdom & Holman 1991; Wisdom 2006), following the methodology described by Kane & Raymond (2014), Kane (2019, 2023b), and Kane et al. (2021b).

Two main simulation suites were conducted; one for the "Jupiter analog" case that adopts the present Jupiter eccentricity of 0.049, and one for the "eccentric Jupiter" case that adopts the median eccentricity of giant planets beyond the snow line of 0.23 (see Section 2.2). A Jupiter mass and solar mass were adopted for the planetary and star masses, respectively, and the semimajor axis of the planet was set to 5.2 au. The simulations within each suite explored a location range of 3.0–8.0 au in steps of 0.01 au, resulting in ∼500 simulations for each of the simulation suites. The simulations at each semimajor axis step were run for 10^5 yr with a time step of 10 days. At each semimajor axis location, 100 particles, each with a mass of 10^{-6} Earth masses, were injected into circular orbits at equally spaced starting locations. At the conclusion of the simulation for a given semimajor axis location, the "scattering efficiency" of the planet for the specified location is calculated from the percentage of particles that, at any point during the simulation, are scattered into an orbit whose periastron location is interior to the snow line ($q = a_{\rm ice} = 2.7$ au) or Earth's orbit ($q = 1.0$ au). The data from all simulations for both suites were then compiled for the subsequent analysis.

The particle injection simulation data are represented within the panels shown in Figure 2, where the scattering efficiency results for the Jupiter analog and eccentric Jupiter cases are shown in the top and bottom panels, respectively. The solid and dotted lines indicate scattering interior to the snow line and Earth orbit, respectively. The gray vertical dashed line indicates

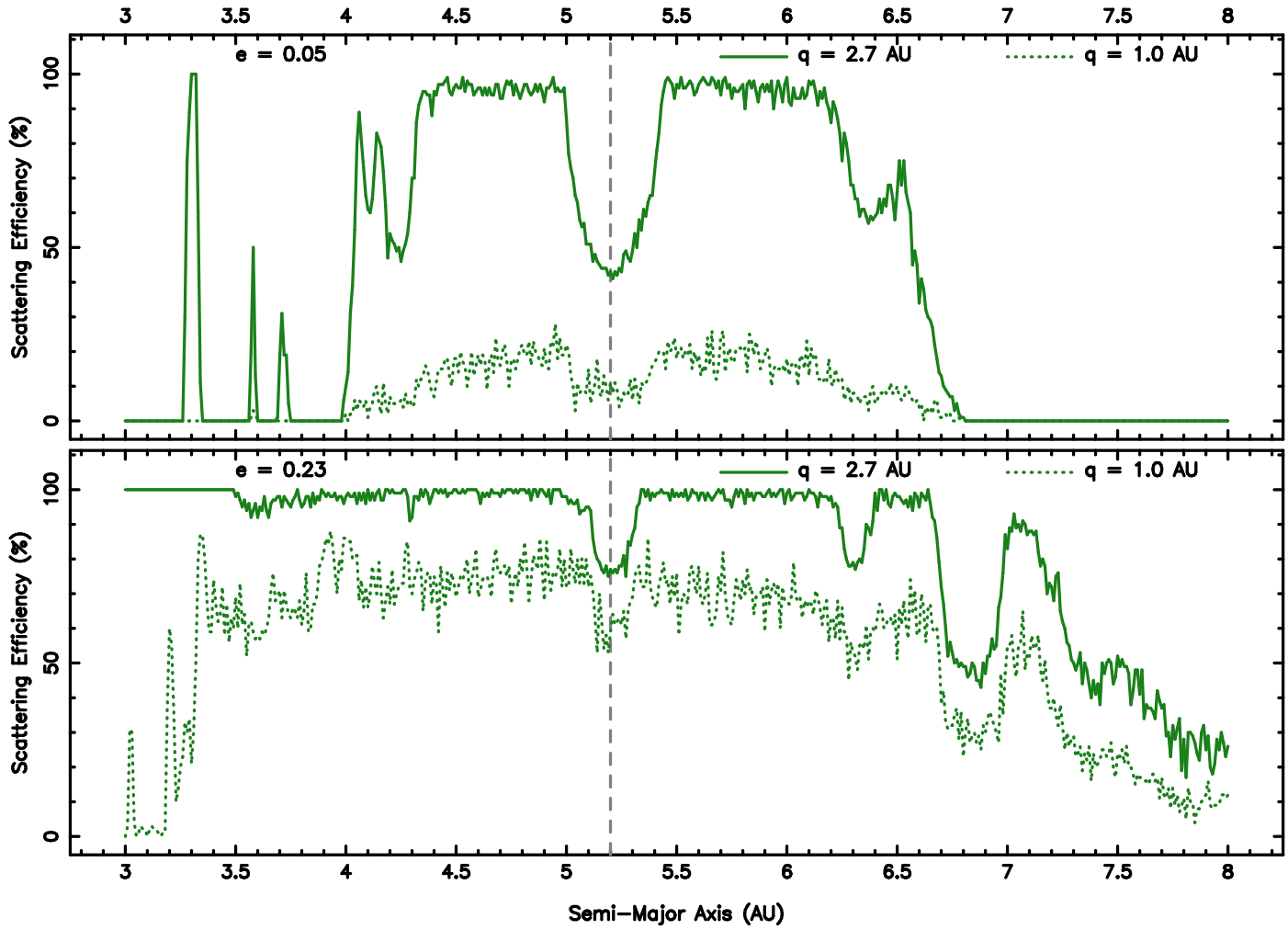

Figure 2. Results for the particle injection simulation that tests the scattering efficiency of a Jupiter analog ($e = 0.05$; top panel) compared with an enhanced eccentricity Jupiter ($e = 0.23$; bottom panel). For each panel, results are plotted for the percentage of particles that achieve periastron passages interior to the snow line ($q = 2.7$ au; solid line) and interior to an Earth orbit ($q = 1.0$ au; dotted line). The gray vertical dashed line indicates the semimajor axis of the giant planet.

the semimajor axis of the giant planet. For each case, and by definition, the scattering efficiency interior to Earth's orbit is a subset of that interior to the snow line. Both cases also show the same reduction in scattering efficiency near the planetary semimajor axis of 5.2 au due to the relative stability of Trojan particles (Levison et al. 1997; Morbidelli et al. 2005; Nesvorný et al. 2013; Bottke et al. 2023). The Jupiter analog case, shown in the top panel, clearly exhibits enhanced scattering potential at locations of mean motion resonance (MMR), particularly for the 2:1 (∼3.2 au), 7:4 (∼3.6 au), and 5:3 (∼3.7 au) MMR locations. Locations of MMR become less efficient at scattering when at larger semimajor axis locations due to the less frequent gravitational perturbations from the planet. The eccentric Jupiter case, shown in the bottom panel, produces similar MMR effects, but the scattering potential of the planet is so enhanced by the change in orbital eccentricity that the MMR locations are not nearly as obvious as they are for the Jupiter analog case.

In general, the scattering efficiency of the Jupiter analog case is less than that for the eccentric Jupiter case for the full range of particle locations. For the Jupiter analog case, 43.6% and 7.0% of particles are scattered interior to the snow line and Earth's orbit, respectively, when integrated over all particle locations. For the eccentric Jupiter case, 84.5% and 54.7% of particles are scattered interior to the snow line and Earth's orbit, respectively. These simulation results lead to the conclusion that the eccentric Jupiter scatters almost double (factor of 1.9) the amount of material interior to the snow line, and 7.8 times the amount of material into Earth-crossing orbits, compared with the Jupiter analog case. However, it is worth considering that the vast majority of planetesimal material within the "feeding zone" of the giant planet will have been significantly depleted during the formation of the planet (Pollack et al. 1996; Alibert et al. 2005). To account for this, we repeated the above scattering calculations, integrated over all locations but excluding material within three Hill radii (±1 au) of the planetary semimajor axis (Raymond & Izidoro 2017). For the Jupiter analog case, the revised total scattering efficiencies are 16.7% and 1.6% for the snow line and Earth's orbit, respectively. For the eccentric Jupiter case, the revised total scattering efficiencies are 76.5% and 43.7% for the snow line and Earth's orbit, respectively. Insofar as the scattered material contains volatiles, most particularly water, then the above-described perturbative effects of the giant planet will likely provide a significantly greater opportunity for building the water inventory of inner terrestrial planets.

4. Discussion

Searches for exoplanets have always been influenced by a deep human desire to understand the context for the solar system's orbital configuration and, in recent decades, we have learned much about the frequency with which the Universe produces planetary systems of various architectures. As described in Section 1, a key characteristic of our solar system is the presence of long-period, cold giant planets. Long-duration RV surveys with decades of observations have revealed that such planets are present around ∼10% of stars (e.g., Cumming et al. 2008; Wittenmyer et al. 2011, 2020; Fulton et al. 2021; Bonomo et al. 2023). In terms of potential solar system analogs, Wittenmyer et al. (2016) derived an occurrence rate of $6.2^{+2.8}_{-1.6}$% for systems containing a low-eccentricity ($e < 0.2$) Jupiter analog and no interior giant planets. The connection between cold Jupiters and inner super-Earths has also been explored at length. Recent results are in general agreement that those two types of planets appear to be correlated (e.g., Zhu & Wu 2018; Bryan et al. 2019; Rosenthal et al. 2022), with nearly all cold-Jupiter systems thought to also host interior super-Earths (but see Bonomo et al. 2023 for a counterargument). However, as our solar system contains no super-Earths, it may be more relevant to consider the frequency of systems containing a cold Jupiter and no super-Earths.

The astrobiological importance in understanding the occurrence of cold Jupiters is primarily related to their relationship to the volatile delivery and the water inventory of inner, terrestrial planets (Raymond et al. 2004; Raymond & Bonsor 2014; Ciesla et al. 2015; Raymond & Izidoro 2017; Marov & Ipatov 2018; Venturini et al. 2020). Methods are actively being developed to detect high-water-content atmospheres, potentially indicative of a water-dominated surface, from current transmission spectroscopic data (Kempton et al. 2023). The accumulation of such significant atmospheric water detections will provide a statistical context to possible water delivery from beyond the snow line, and thus a means to test the various scenarios proposed for such delivery. Indeed, the volatile inventory of inner planets can test the location of the snow line with respect to pebble accretion scenarios (Bitsch et al. 2021). It is worth noting that the nature and volume of volatile scattering that originates from giant planet perturbations also depends on the distribution of volatiles throughout the protoplanetary disk (Pollack et al. 1996; Lodders 2003; Artur de la Villarmois et al. 2019; Öberg & Bergin 2021). Our scattering efficiency results may be effectively scaled to the known or inferred distribution of volatiles within a particular planetary system.

The results described in Section 3 show that the median exoplanetary architecture with a giant planet beyond the snow line is considerably more efficient at scattering volatiles interior to the snow line, particularly to terrestrial planets that may reside within the HZ. The main implication of these results are that water-rich worlds may be more common in those systems with eccentric cold Jupiters, where those terrestrial planets may contain 1 order of magnitude or more water than Earth. This may not necessarily be beneficial for habitability since research by Glaser et al. (2020) showed that the immense seafloor pressures of water worlds can truncate geochemical cycles that transport bioessential elements, such as phosphorus, to ocean chemistry reactions. However, a counterargument by Kite & Ford (2018) is that geochemical cycles with the mantle may not be necessary when the needed bioessential element inventories are acquired via early water–rock interactions with the planetary crust. Water world environments may even be possible for planets that would normally be considered mini-Neptunes (Madhusudhan et al. 2021), although such planets are unlikely to be able to retain water in a liquid state due to water vapor participation in a runaway greenhouse (Innes et al. 2023). Clearly, there remain numerous questions regarding the nature of water worlds, including their origin, their prevalence, and their correlation with the presence of cold giant planetary companions.

A further consideration is that it has been suggested from observational data that giant planets are relatively rare around M dwarfs (Endl et al. 2006; Cumming et al. 2008; Johnson et al. 2010; Bonfils et al. 2013). Considering that M dwarfs are exceptionally common, both intrinsically and as exoplanet targets for follow-up observations, the relative lack of giant planets in these systems may require that other, accretion-related, processes dominate the establishment of a minimum water inventory for HZ planets (Marty 2012; Sato et al. 2016). Some formation models (Lissauer 2007; Menou 2013; Tian & Ida 2015) and observational data (Rogers et al. 2023) support the notion that M dwarf terrestrial planets may indeed be relatively dry. Additionally, planet formation simulations conducted by Raymond et al. (2007) found that it may be difficult for M dwarf accretion disks to form terrestrial planets larger than $\sim 0.3\,M_{\oplus}$, potentially decreasing the probability of M dwarfs participating in habitable planet formation. Alternatively, M dwarf planets that form beyond the snow line and migrate inward may retain substantial water content on the crust and in the mantle (Ogihara & Ida 2009; Unterborn et al. 2018; Pan et al. 2022). Furthermore, ice-rich planetary embryos may migrate interior to the snow line that would otherwise have been blocked by the presence of a giant planet (Izidoro et al. 2015; Bitsch & Savvidou 2021). There are numerous other particular considerations regarding planet formation around M dwarfs, including pebble accretion and disk heating, that are required for a full assessment of the expected water inventory (Adams et al. 2005; Kennedy et al. 2007). Given the diversity of scenarios and associated models for the formation and evolution of terrestrial planets around M dwarfs, further observational evidence is necessary to establish the influence of their formation environment and the role of giant planets (or lack thereof) in their volatile inventory (Tarter et al. 2007).

There are several caveats to note regarding the work presented in this Letter. First, it is worth addressing if there is an observational bias in our sample selection. As noted in Section 2.2, there is certainly an observational bias against the detection of low-mass planets at long periods, but the detection of Saturn-mass and above, as was used for our sample, is largely dominated by the RV survey duration. Those surveys described above generally have sufficient duration and RV precision to establish completeness to the snow lines of the stars monitored, and often considerably further. Our use of Saturn for the planet mass criteria was chosen as a conservative estimate to minimize such completeness issues for the long period planet population considered. We found lowering the mass criteria below $0.1\,M_{\rm J}$ rapidly reaches the detection limit of surveys and so does not alter the median eccentricity of 0.23 for planets beyond the snow line. Second, the choice of 10^5 yr for each simulation duration is sufficient to effectively estimate the majority of scattering events at each semimajor axis location, with the exception of the outer semimajor axis range (as noted

in Section 3). Increasing the duration of simulations would narrow the regions of stability as more gravitational perturbations are accounted for. Third, scattering particles interior to the snow line, or even to an orbit that crosses that of an inner planet, does not translate linearly into impact rates, and thus volatile delivery for the inner planet. Though opportunities for impacts become available with orbit-crossing events, the impact rates are generally proportional to the cross-sectional area of the planet (Horner & Jones 2008). Fourth, there are numerous potential sources for Earth's water inventory aside from that described here (Morbidelli et al. 2012). For example, Ikoma & Genda (2006) suggest that Earth gained substantial water from the nebula during formation via oxidation of a hydrogen-rich atmosphere. Delsemme (1992a, 1992b) proposed a cometary origin for the bulk of Earth's water, but this proposition has been found to be inconsistent with the D/H ratio measurements obtained from long-period comets, which is about twice that for Earth's water (Balsiger et al. 1995). For material scattered by the giant planets, Martin & Livio (2021) estimated that very little of Earth's water originated from beyond the snow line with Jupiter at its present location. However, moving Jupiter to the snow line can produce significant increases in terrestrial planet water delivery, emphasizing the importance of accounting for giant planet migration scenarios (Darriba et al. 2017). Indeed, much of the scattered material by Jupiter and Saturn may have consisted of water-rich primitive asteroidal material (C-type asteroids) at the outer main belt, which in turn may have been populated from a broad range of distances beyond the snow line (Raymond et al. 2009b; Raymond & Izidoro 2017). With all of these volatile delivery factors combined, it is difficult to say in absolute terms how much of the terrestrial planet inventory originates from scattering via giant planets beyond the snow line. However, our simulations demonstrate that it is possible to calculate the relative effects of giant planets on volatile scattering with respect to eccentricity, and the implications derived from the exoplanet eccentricity distribution.

5. Conclusions

Giant planets are a crucial piece of the planetary habitability puzzle since they are often (as in the case of Jupiter) the dominant planetary mass within the system and thus their gravitational effects profoundly influences the system evolution. These influences include the sculpting of the planetary architecture and the distribution and scattering of volatiles that predominantly lie beyond the system snow line. Given that cold giant planets are relatively rare, the lack of their influences within the majority of planetary systems requires careful attention when placing our solar system in a similar context. In this Letter, we have demonstrated that giant planets beyond the snow line have a median eccentricity of 0.23, at least to the limit of current RV survey durations. This median eccentricity is considerably higher than the 0.05 eccentricity of Jupiter. Our dynamical simulations show that, for the solar case, a median eccentricity Jupiter is able to scatter material to the inner part of the planetary system substantially more efficiently than the Jupiter analog case. Specifically, the scattering efficiency is increased by factors of 1.9 and 7.8 for material reaching interior to the snow line and Earth-crossing orbit, respectively. This implies that most systems with giant planets beyond the snow line may play an even more important role in distributing volatiles to the inner terrestrial planets than Jupiter did in our system, and indeed the prevalence of water worlds may be greater in the presence of such cold eccentric Jupiters as a result. This prediction may be tested through the detection of atmospheric water vapor and bulk planetary densities that allow the inference of volatile inventories for a wide range of planetary architectures.

Acknowledgments

The authors would like to thank Sean Raymond for his valuable feedback on the manuscript. This research has made use of the NASA Exoplanet Archive, which is operated by the California Institute of Technology, under contract with the National Aeronautics and Space Administration under the Exoplanet Exploration Program. This research has also made use of the Habitable Zone Gallery at http://hzgallery.org. The results reported herein benefited from collaborations and/or information exchange within NASA's Nexus for Exoplanet System Science (NExSS) research coordination network sponsored by NASA's Science Mission Directorate.

Software: Mercury (Chambers 1999).

ORCID iDs

Stephen R. Kane https://orcid.org/0000-0002-7084-0529
Robert A. Wittenmyer https://orcid.org/0000-0001-9957-9304

References

Adams, F. C., Bodenheimer, P., & Laughlin, G. 2005, AN, 326, 913
Akeson, R. L., Chen, X., Ciardi, D., et al. 2013, PASP, 125, 989
Alibert, Y., Mordasini, C., Benz, W., & Winisdoerffer, C. 2005, A&A, 434, 343
Artur de la Villarmois, E., Jørgensen, J. K., Kristensen, L. E., et al. 2019, A&A, 626, A71
Balsiger, H., Altwegg, K., & Geiss, J. 1995, JGR, 100, 5827
Bitsch, B., Raymond, S. N., Buchhave, L. A., et al. 2021, A&A, 649, L5
Bitsch, B., & Savvidou, S. 2021, A&A, 647, A96
Bonfils, X., Delfosse, X., Udry, S., et al. 2013, A&A, 549, A109
Bonomo, A. S., Dumusque, X., Massa, A., et al. 2023, A&A, 677, A33
Bottke, W. F., Marschall, R., Nesvorný, D., & Vokrouhlický, D. 2023, SSRv, 219, 83
Bryan, M. L., Knutson, H. A., Lee, E. J., et al. 2019, AJ, 157, 52
Chambers, J. E. 1999, MNRAS, 304, 793
Ciesla, F. J. 2014, ApJL, 784, L1
Ciesla, F. J., Mulders, G. D., Pascucci, I., & Apai, D. 2015, ApJ, 804, 9
Clement, M. S., Quintana, E. V., & Quarles, B. L. 2022, ApJ, 928, 91
Clement, M. S., Raymond, S. N., Kaib, N. A., et al. 2021, Icar, 355, 114122
Cumming, A., Butler, R. P., Marcy, G. W., et al. 2008, PASP, 120, 531
Darriba, L. A., de Elía, G. C., Guilera, O. M., & Brunini, A. 2017, A&A, 607, A63
Delsemme, A. H. 1992a, OLEB, 21, 279
Delsemme, A. H. 1992b, AdSpR, 12, 5
Endl, M., Cochran, W. D., Kürster, M., et al. 2006, ApJ, 649, 436
Fischer, D. A., Anglada-Escude, G., Arriagada, P., et al. 2016, PASP, 128, 066001
Ford, E. B. 2008, AJ, 135, 1008
Ford, E. B. 2014, PNAS, 111, 12616
Ford, E. B., & Rasio, F. A. 2008, ApJ, 686, 621
Fulton, B. J., Rosenthal, L. J., Hirsch, L. A., et al. 2021, ApJS, 255, 14
Glaser, D. M., Hartnett, H. E., Desch, S. J., et al. 2020, ApJ, 893, 163
Goldreich, P., & Soter, S. 1966, Icar, 5, 375
He, M. Y., Ford, E. B., & Ragozzine, D. 2019, MNRAS, 490, 4575
Hill, M. L., Bott, K., Dalba, P. A., et al. 2023, AJ, 165, 34
Hill, M. L., Kane, S. R., Seperuelo Duarte, E., et al. 2018, ApJ, 860, 67
Hogg, D. W., Myers, A. D., & Bovy, J. 2010, ApJ, 725, 2166
Horner, J., & Jones, B. W. 2008, IJAsB, 7, 251
Horner, J., Kane, S. R., Marshall, J. P., et al. 2020, PASP, 132, 102001
Ida, S., & Lin, D. N. C. 2005, ApJ, 626, 1045
Ida, S., Lin, D. N. C., & Nagasawa, M. 2013, ApJ, 775, 42

Ikoma, M., & Genda, H. 2006, ApJ, 648, 696
Innes, H., Tsai, S.-M., & Pierrehumbert, R. T. 2023, ApJ, 953, 168
Ivanov, P. B., & Papaloizou, J. C. B. 2007, MNRAS, 376, 682
Izidoro, A., Raymond, S. N., Morbidelli, A., Hersant, F., & Pierens, A. 2015, ApJL, 800, L22
Johnson, J. A., Aller, K. M., Howard, A. W., & Crepp, J. R. 2010, PASP, 122, 905
Jones, H. R. A., Butler, R. P., Tinney, C. G., et al. 2006, MNRAS, 369, 249
Jurić, M., & Tremaine, S. 2008, ApJ, 686, 603
Kane, S. R. 2011, Icar, 214, 327
Kane, S. R. 2015, ApJL, 814, L9
Kane, S. R. 2019, AJ, 158, 72
Kane, S. R. 2023a, PSJ, 4, 38
Kane, S. R. 2023b, AJ, 166, 187
Kane, S. R., Arney, G. N., Byrne, P. K., et al. 2021a, JGRE, 126, e06643
Kane, S. R., Ciardi, D. R., Gelino, D. M., & von Braun, K. 2012, MNRAS, 425, 757
Kane, S. R., & Gelino, D. M. 2012, PASP, 124, 323
Kane, S. R., Hill, M. L., Kasting, J. F., et al. 2016, ApJ, 830, 1
Kane, S. R., Li, Z., Wolf, E. T., Ostberg, C., & Hill, M. L. 2021b, AJ, 161, 31
Kane, S. R., & Raymond, S. N. 2014, ApJ, 784, 104
Kane, S. R., Schneider, D. P., & Ge, J. 2007, MNRAS, 377, 1610
Kane, S. R., Turnbull, M. C., Fulton, B. J., et al. 2020, AJ, 160, 81
Kasting, J. F., Whitmire, D. P., & Reynolds, R. T. 1993, Icar, 101, 108
Kempton, E. M. R., Lessard, M., Malik, M., et al. 2023, ApJ, 953, 57
Kennedy, G. M., & Kenyon, S. J. 2008, ApJ, 673, 502
Kennedy, G. M., Kenyon, S. J., & Bromley, B. C. 2006, ApJL, 650, L139
Kennedy, G. M., Kenyon, S. J., & Bromley, B. C. 2007, Ap&SS, 311, 9
Kite, E. S., & Ford, E. B. 2018, ApJ, 864, 75
Kopparapu, R. K., & Barnes, R. 2010, ApJ, 716, 1336
Kopparapu, R. K., Ramirez, R., Kasting, J. F., et al. 2013, ApJ, 765, 131
Kopparapu, R. K., Ramirez, R. M., SchottelKotte, J., et al. 2014, ApJL, 787, L29
Levison, H. F., Shoemaker, E. M., & Shoemaker, C. S. 1997, Natur, 385, 42
Lissauer, J. J. 2007, ApJL, 660, L149
Lodders, K. 2003, ApJ, 591, 1220
Madhusudhan, N., Piette, A. A. A., & Constantinou, S. 2021, ApJ, 918, 1
Marov, M. Y., & Ipatov, S. I. 2018, SoSyR, 52, 392
Martin, R. G., & Livio, M. 2015, ApJ, 810, 105
Martin, R. G., & Livio, M. 2021, MNRAS, 506, L6
Marty, B. 2012, E&PSL, 313, 56
Menou, K. 2013, ApJ, 774, 51
Mishra, L., Alibert, Y., Udry, S., & Mordasini, C. 2023, A&A, 670, A68
Morbidelli, A., Chambers, J., Lunine, J. I., et al. 2000, M&PS, 35, 1309
Morbidelli, A., Levison, H. F., Tsiganis, K., & Gomes, R. 2005, Natur, 435, 462
Morbidelli, A., Lunine, J. I., O'Brien, D. P., Raymond, S. N., & Walsh, K. J. 2012, AREPS, 40, 251
Morbidelli, A., & Raymond, S. N. 2016, JGRE, 121, 1962
Morbidelli, A., Tsiganis, K., Crida, A., Levison, H. F., & Gomes, R. 2007, AJ, 134, 1790
NASA Exoplanet Archive 2023, Planetary Systems, Version: 2023-10-20, NExScI-Caltech/IPAC, doi:10.26133/NEA12
Nesvorný, D., Vokrouhlický, D., & Morbidelli, A. 2013, ApJ, 768, 45
Öberg, K. I., & Bergin, E. A. 2021, PhR, 893, 1
Ogihara, M., Genda, H., & Sekine, Y. 2023, PSJ, 4, 32
Ogihara, M., & Ida, S. 2009, ApJ, 699, 824
Pan, M., Wang, S., & Ji, J. 2022, MNRAS, 510, 4134
Pollack, J. B., Hubickyj, O., Bodenheimer, P., et al. 1996, Icar, 124, 62
Raymond, S. N. 2006, ApJL, 643, L131
Raymond, S. N., Armitage, P. J., & Gorelick, N. 2009a, ApJL, 699, L88
Raymond, S. N., Armitage, P. J., & Gorelick, N. 2010, ApJ, 711, 772
Raymond, S. N., Barnes, R., Armitage, P. J., & Gorelick, N. 2008, ApJL, 687, L107
Raymond, S. N., & Bonsor, A. 2014, MNRAS, 442, L18
Raymond, S. N., & Izidoro, A. 2017, Icar, 297, 134
Raymond, S. N., Izidoro, A., & Morbidelli, A. 2020, in Planetary Astrobiology, ed. V. S. Meadows et al. (Tucson, AZ: Univ. Arizona Press), 287
Raymond, S. N., O'Brien, D. P., Morbidelli, A., & Kaib, N. A. 2009b, Icar, 203, 644
Raymond, S. N., Quinn, T., & Lunine, J. I. 2004, Icar, 168, 1
Raymond, S. N., Scalo, J., & Meadows, V. S. 2007, ApJ, 669, 606
Ribas, I., & Miralda-Escudé, J. 2007, A&A, 464, 779
Rogers, J. G., Schlichting, H. E., & Owen, J. E. 2023, ApJL, 947, L19
Rosenthal, L. J., Fulton, B. J., Hirsch, L. A., et al. 2021, ApJS, 255, 8
Rosenthal, L. J., Knutson, H. A., Chachan, Y., et al. 2022, ApJS, 262, 1
Sagear, S., & Ballard, S. 2023, PNAS, 120, e2217398120
Sato, T., Okuzumi, S., & Ida, S. 2016, A&A, 589, A15
Shen, Y., & Turner, E. L. 2008, ApJ, 685, 553
Tarter, J. C., Backus, P. R., Mancinelli, R. L., et al. 2007, AsBio, 7, 30
Tian, F., & Ida, S. 2015, NatGe, 8, 177
Unterborn, C. T., Desch, S. J., Hinkel, N. R., & Lorenzo, A. 2018, NatAs, 2, 297
Venturini, J., Ronco, M. P., & Guilera, O. M. 2020, SSRv, 216, 86
Winn, J. N., & Fabrycky, D. C. 2015, ARA&A, 53, 409
Wisdom, J. 2006, AJ, 131, 2294
Wisdom, J., & Holman, M. 1991, AJ, 102, 1528
Wittenmyer, R. A., Butler, R. P., Tinney, C. G., et al. 2016, ApJ, 819, 28
Wittenmyer, R. A., Tinney, C. G., Horner, J., et al. 2013, PASP, 125, 351
Wittenmyer, R. A., Tinney, C. G., O'Toole, S. J., et al. 2011, ApJ, 727, 102
Wittenmyer, R. A., Wang, S., Horner, J., et al. 2020, MNRAS, 492, 377
Wright, J. T., Upadhyay, S., Marcy, G. W., et al. 2009, ApJ, 693, 1084
Zhu, W., & Wu, Y. 2018, AJ, 156, 92